



E93 expression and links to the juvenile hormone in hemipteran mealybugs with insights on female neoteny

Isabelle Mifom Veal^{a,b,*}, Sayumi Tanaka^a, Tomohiro Tsuji^a, Takahiro Shiotsuki^{c,d}, Akiya Jouraku^c, Chieka Minakuchi^a

^a Nagoya University, Graduate School of Bioagricultural Sciences, Nagoya, Japan

^b University of Edinburgh, Institute of Evolutionary Biology, Edinburgh, UK

^c Institute of Agrobiological Sciences, National Institute of Agriculture and Food Research Organization, Tsukuba, Japan

^d Shimane University, Faculty of Life and Environmental Science, Matsue, Japan

ARTICLE INFO

Keywords:

E93
Insect metamorphosis
Neoteny
Hemimetaboly
Juvenile hormone
Mealybugs

ABSTRACT

Insect metamorphosis produces reproductive adults and is commonly accompanied with the direct or indirect development of wings. In some winged insects, the imago is altered by life history changes. For instance, in scale insects and mealybugs, reproductive females retain juvenile features and are wingless. The transcription factor *E93* triggers metamorphosis and plays in concert with the juvenile hormone pathway to guarantee the successful transition from juvenile to adult. We previously provided evidence of an atypical down-regulation of the juvenile hormone pathway during female development in the Japanese mealybug. Here, we further investigate how *E93* is involved in the production of neotenic wingless females, by identifying its isoforms, assessing their expression patterns and evaluating the effect of exogenous juvenile hormone mimic treatment on *E93*. This study identifies three *E93* isoforms on the 5' end, based on Japanese mealybug cDNA and shows that female development occurs with the near absence of *E93* transcripts, as opposed to male metamorphosis. Additionally, while male development is typically affected by exogenous juvenile hormone mimic treatments, females seem to remain insensitive to the treatment, and up-regulation of the juvenile hormone signaling is not observed. Furthermore, juvenile hormone mimic treatment on female nymphs did not have an obvious effect on *E93* transcription, while treatment on male prepupae resulted in depleted *E93* transcripts. In this study, we emphasize the importance in examining atypical cases of metamorphosis as complementary systems to provide a better understanding on the molecular mechanisms underlying insect metamorphosis. For instance, the factors regulating the expression of *E93* are largely unclear. Investigating the regulatory mechanism of *E93* transcription could provide clues towards identifying the factors that induce or suppress *E93* transcription, in turn triggering male adult development or female neoteny.

1. Introduction

The evolution of metamorphosis undeniably contributed to the diversity of insect forms, life histories and increased opportunities for ecological niche exploitation (Grimaldi and Engel, 2005; Truman and Riddiford, 1999). While two types of metamorphosis – holometaboly and hemimetaboly – predominate in insects, in a few lineages, life cycles deviate to form unusual developmental instances, nonetheless leading to important adaptations. For example, hypermetamorphosis, manifested by two types of larvae, arose from holometaboly. Found in Strepsiptera, Meloidae and Rhipiphoridae beetles, neuropteran Mantispidae and many Hymenoptera and some Diptera,

hypermetamorphosis is often associated to parasitic life (Truman and Riddiford, 2002) or predatory habits (Belles, 2011). Neometaboly is another metamorphosis found in plant sap-feeding hemimetabolous Paraneoptera (Aleyrodoidea, Thysanoptera, and male Coccoomorpha), in which the formation of quiescent stages ("prepupae" and "pupae") is reminiscent to holometaboly (Belles, 2011; Sehnaal et al., 1996).

Two hormones orchestrate insect metamorphosis: ecdysone and the juvenile hormone (JH). JH, in particular, dictates the identity of subsequent stages and is therefore of special interest for understanding how peculiar life cycles arise. An essential player, the transcription factor *E93*, triggers adult metamorphosis and is universally up-regulated at the end of insect juvenile development (Ureña et al., 2014). *E93*

* Corresponding author. University of Edinburgh, Institute of Evolutionary Biology, Edinburgh, UK.
E-mail address: isabelle.vea@gmail.com (I.M. Veal).

<https://doi.org/10.1016/j.ibmb.2018.11.008>

Received 16 March 2018; Received in revised form 28 November 2018; Accepted 28 November 2018

Available online 29 November 2018

0965-1748/ © 2018 Elsevier Ltd. All rights reserved.

involvement was first reported in *Drosophila melanogaster* cell death process in the prepupa (Baehrecke and Thummel, 1995; Buszczak and Segraves, 2000; Lee et al., 2000) and acts as a developmental switch to control the responsiveness of target genes during metamorphosis (Mou et al., 2012). Later, functional studies on *E93* orthologs in both hemimetabolous and holometabolous species confirmed *E93* is a universal adult specifier in insect metamorphosis (Ureña et al., 2014). Finally, a communication between *E93* and JH signaling pathway exists (Jindra et al., 2015). In fact, *Krüppel homolog 1* (*Kr-h1*), an early response gene of JH signaling, acts as a repressor of *E93* until the onset of adult metamorphosis: knocking down *Kr-h1* at the penultimate juvenile instar of hemimetabolous *Blattella germanica* results in the early increase of *E93* (Belles and Santos, 2014). Thereafter, functional studies in hemimetabolous *Cimex lectularius* (Gujar and Palli, 2016) and *Tribolium castaneum* pupal stage (Ureña et al., 2016) confirmed the interaction of JH signaling and *E93* in other insect lineages. Finally, the direct transcriptional repressor role of *Kr-h1* on *E93* promoter region was confirmed in *Bombyx mori* (Kayukawa et al., 2017).

Some unusual life cycle alterations can also result in reproductive forms retaining juvenile features: neoteny. Considered merely as curiosities, neotenic forms originated multiple times in various insects and can be associated to particular adaptive traits. Examples include parasitism in Strepsiptera (Kathirithamby, 2009), Isoptera sociality (Higashi and Abe, 1997; Roisin, 2000), and bioluminescence-generating Elateriformia (fireflies, jewel beetles, click beetles etc...) (Bocakova et al., 2007; South et al., 2011). Nevertheless, few studies have addressed the underlying molecular mechanisms of neoteny. The emergence of diverse ways to metamorphose could be associated to the change in maturation timing (heterochrony), which implies that variations in controlling hormones may be an essential factor in establishing these forms (Gould, 1977). As such, female-specific neotenic forms could be tightly linked to the reproductive functions of JH (see review of JH signaling in reproduction (Roy et al., 2018)). So far, the main hypothesis for the creation of juvenile-like reproductive females resides in excessive levels of JH, simultaneously affecting female developmental progress and the timing of activating reproductive function (Matsuda, 1976).

Excessive JH titers are indeed observed in termite neotenic forms of *Reticulitermes speratus*. Here, the female reproductive neotenic caste shows significantly higher JH titers than those of the nymphs or worker castes. Additionally, knocking down JH receptor (*RsMet*) depletes *vitellogenin* transcript levels. However, it is still unclear whether the phenotypic features attributed to neotenic forms are affected (Saiki et al., 2015). The only other molecular studies on insect neotenic forms were undertaken on holometabolous insects, where the role of ecdysone was investigated as the responsible factor. Strepsiptera (twisted-wing insects) display sex-specific neotenic forms, whereby females in extreme groups are larviform and endoparasitic. The expression patterns of the pupal specifier *broad* in *Xenos vesparum* was also examined. In holometabolous insects, *broad* is up-regulated during the last larval instar, at the onset of metamorphosis with an ecdysone titer increase (Kiss et al., 1988; Konopova and Jindra, 2008; Parthasarathy et al., 2008; Uhlirova et al., 2003). In *X. vesparum*, only males that undergo metamorphosis showed the increase of *broad* BTB domain expression, while it was not observed in last larval instar females (Erezyilmaz et al., 2014). Finally, Cecidomyiidae (gall midges) possess a facultative paedogenetic life cycle where ovaries differentiate and grow precociously in the larval stage. In this instance, a shift in timing of *ecdysone receptor* and *ultraspiracle* expression kick-starts the facultative life cycle and creates larval reproductive females (Hodin and Riddiford, 2000).

Scale insects and mealybugs (Coccoomorpha) belong to Hemiptera, an insect order that mostly develop through hemimetaboly. However, Coccoomorpha species have departed from the traditional nymphal instars with progressive wing growth. Males undergo two quiescent stages reminiscent to complete metamorphosis (neometaboly, as mentioned above). In striking contrast, reproductive females retain juvenile

features, as they develop through successive molts without wing growth, reduction of nymphal stage number and features linked to mobility in many species. This life history trait not only gives rise to extremely sexually dimorphic organisms, but offers a successful strategy, as plant-sap feeding insects, to allocate energy to reproduction, adopt a sedentary life, driving the reduction of appendages, change of body shapes and creation of different defensive secretions to adapt to their host-plant habitats (Gullan and Kosztarab, 1997). Female scale insects and mealybugs are often described as neotenic (Danzig, 1980; Koteja, 1990). However, which type of neoteny, or the mechanisms by which adult females keep juvenile features remains unknown. This prevents us from understanding the link between the development and evolution of neoteny. More importantly, this lineage includes some of the most damaging agricultural pests in human activities, likely a consequence of the evolution of neotenic females and their adaptive life history to host plants.

We previously presented a study on the variation of JH signaling in the Japanese mealybug *Planococcus kraunhiae* (Kuwana) (Pseudococcidae) to examine distinctive gene expression patterns between male and female development as a possible mechanism leading to extreme sexual dimorphism in scale insects. In addition to significant differences in JH early-response gene *Kr-h1* when male and female mealybugs start to differentiate, we reported that JH signaling remained unusually low throughout female adult development, suggesting a contrasting JH regulation of female neoteny (Veá et al., 2016). To further examine the involvement of *E93* in female neoteny, in relation to the JH signaling, we compare the expression pattern of *E93*, in *P. kraunhiae* male and female postembryonic development and perform hormonal assays using a JH mimic, pyriproxyfen. We hypothesize that in scale insects, females fail to express *E93*, resulting in the maintenance of juvenile features in their external morphology even after reproductive maturation. Additionally, we test whether increasing levels of JH during the last nymphal instar in females readjusts the expression of *Kr-h1* at similar levels as seen in males, which in turn could allow to initiate *E93* expression. It turns out that females are insensitive to exogenous JHM treatment in the context of the effects on *Kr-h1* and *E93* expression as well as on adult development.

2. Materials and methods

2.1. Mealybug rearing and sampling strategy

Mealybug culture and sampling strategy for gene expression profile are described in a previous study on JH variations in the *P. kraunhiae* (Veá et al., 2016). In the current study, we carried out an independent sampling to ensure reproducibility of the previous study. As such, we collected samples every 24 h after oviposition. Eggs oviposited during the first day were used for male-biased samples and eggs oviposited during the fifth day for female-biased samples (see Veá et al., 2016 for sex-biased sample strategy). All stages are abbreviated as follows: E = embryonic stage after oviposition, N1 = first-instar nymph, N2 = second-instar nymph, N2f = female second-instar nymph, N2m = male second-instar nymph, N3 = female third-instar nymph, pre = male prepupa, pu = male pupa, m = male adult, f = female adult.

2.2. cDNA cloning and identification of sequences

The total RNA of pooled individuals from different stages was extracted with TRIzol (as described in Veá et al., 2016) and Oligo-dT-primed reverse transcription was performed with the PrimeScript II 1st strand cDNA synthesis kit (Takara Bio, Shiga, Japan). The conserved region of *E93* sequence in *B. germanica* was blasted against a transcriptome of *P. kraunhiae* [DDBJ (DNA databank of Japan, <https://www.ddbj.nig.ac.jp/>)/EMBL-Bank/GenBank accession number DRA004114 (Sugahara et al., 2016)], and primers for RT-PCR were

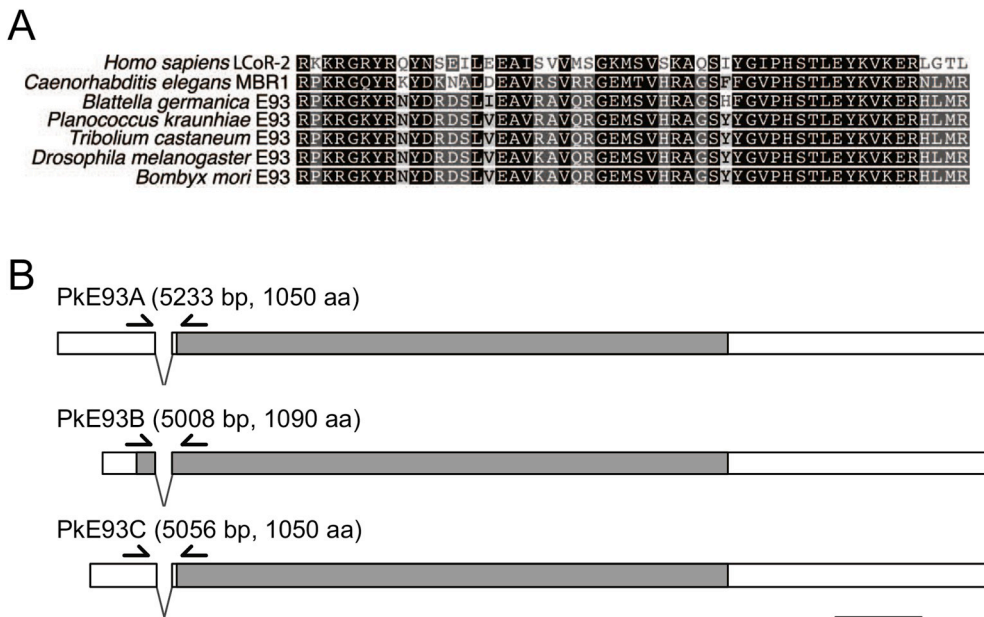


Fig. 1. Identification of PkE93 sequence and the structure of its isoforms. **A.** Amino acid alignment of the Pipsqueak DNA-binding domain with other insects' E93, *Homo sapiens* LCoR-2 and *Caenorhabditis elegans* MBR1 [sequences from (Ureña et al., 2014)]. **B.** General structure of cDNA sequences obtained from 5' and 3' RACE PCR. The sequences are identical on the 3' end, while the 5' end differs among the three isoforms, the common region has 4676 bp starting from 3' end. Grey: open reading frame. Arrows: primers designed for qRT-PCR. Scale bar: 500 bp.

designed to amplify a partial region of the gene. Primers for RACE PCR were designed based on this partial sequence, and 5' and 3' RACE was conducted with SMARTer RACE cDNA Amplification Kit (Takara Bio USA, Inc., Mountain View, CA) in order to retrieve the full-length cDNA sequences. All PCR products were cloned in a pGEM-T Easy Vector (Promega, Madison, WI) and sequenced. DNA sequence data were deposited in the DDBJ/EMBL-Bank/GenBank International Nucleotide Sequence Database with the following accession numbers: *PkE93* isoform A (LC374380), *PkE93* isoform B (LC374381) and *PkE93* isoform C (LC374382). The primer sequences are listed in Table S1.

2.3. RNA extraction and quantitative RT-PCR

Total RNA was extracted from all samples using the sex-biased sampling as described in Vea et al. (2016) and the link to detailed protocol in Appendix A. For the expression profile analysis, each sample consisted of 0.5–2 mg of pooled individuals homogenized in TRIzol reagent, total RNA was extracted using nuclease-free glycogen (Thermo Fisher Scientific) as a carrier, and reverse transcribed using the PrimeScript RT reagent Kit with gDNA Eraser (Takara Bio). Expression profiles for the post-oviposition development of males and females were established by quantifying the levels of transcripts for targeted fragments using absolute quantitative RT-PCR (qRT-PCR), performed on a Thermal Cycler Dice Real Time System (model TP800, Takara Bio) as described previously (Vea et al., 2016). Six serial dilutions from a plasmid containing the target region at 1 ng/μL was used as the standard for each qRT-PCR plate. Primer sequences for each *PkE93* isoform used for qRT-PCR are listed in Table S1. The values obtained by the second derivative maximum (SDM) method were normalized with the ribosomal protein *L32* (*rpl32*) transcript levels. Primers for *PkrpL32*, our reference gene, and *PkKr-h1A* were from our previous study (Vea et al., 2016).

2.4. JH mimic assays on male prepupae and female juvenile instars

For JH mimic (JHM) treatments, we applied 2 μL of pyriproxyfen (5 mM dissolved in methanol) to batches of 3–5 male prepupae on a filter paper, 24–48 h after molting. Excess chemical solution was immediately absorbed by the filter paper. After treatment, we waited for the solvent to evaporate completely before transferring them in 1.5 mL microcentrifuge tubes (Ina Optica, Osaka, Japan), bearing a paper disc (8 mm in diameter, 1.5 mm in thickness; Toyo Roshi, Japan) with 10 μL

of distilled water to control humidity. Female N3D0 (0–24 h after molting to the N3 stage) were treated in the same manner except that 0.5 μL of pyriproxyfen (20 mM dissolved in methanol) was applied on the tergite of individual N3D0. After the N3D0 started to move again, it was transferred into a glass dish containing a sprouted broad bean on top of a filter paper. The glass dishes were sealed with parafilm. Treated samples were left to incubate at 23 °C for various numbers of days after treatment before being homogenized in TRIzol and stored at –80 °C for RNA extraction. RNA extraction, reverse transcription and qRT-PCR analyses were performed as described in 2.3, except that we obtained 3 to 7 biological replicates per treatment and day after treatment (1 biological replicate consists of the RNA extraction from 5 pooled male pupae or a single female). The link to detailed protocol can be found in Appendix A.

2.5. Graphs and statistical analyses

Graphs from qRT-PCR SDM values were generated using the R package ggplot2 (Gómez-Rubio, 2017). All SDM values were normalized with *rpl32* SDM values to obtain relative expression for the gene expression profiles. In the case of effect of treatment, the relative expression was further log₁₀ transformed. To test for statistical significance, we fitted the linear model in R (lm()) on the log₁₀ transformed data to test the significance of pyriproxyfen treatments over time. In the model we considered both treatment and day after treatment as predictors, as well as the interaction between both. The detailed analyses are available on GitHub (<https://doi.org/10.5281/zenodo.1745554>). P-values for each predictor are indicated on top right side of each graph (Figs. 3 and 4). If the interaction is significant, the p-values of predictors treatment (JHM), time (day after treatment: DAT) and interaction between them (JHM:DAT) are indicated (as it is the case for *PkKr-h1*). If no interaction was found, we fitted the linear model excluding the interaction and indicated p-values for treatment and day after treatment only (for all three *PkE93* isoforms). We considered an effect significant when p-value < 0.01.

3. Results and discussion

3.1. Structure of E93 in *P. kraunhiae*

The *PkE93* sequence identified from RT-PCR includes a Pipsqueak DNA binding domain characteristic of *E93* (Siegmond and Lehmann,

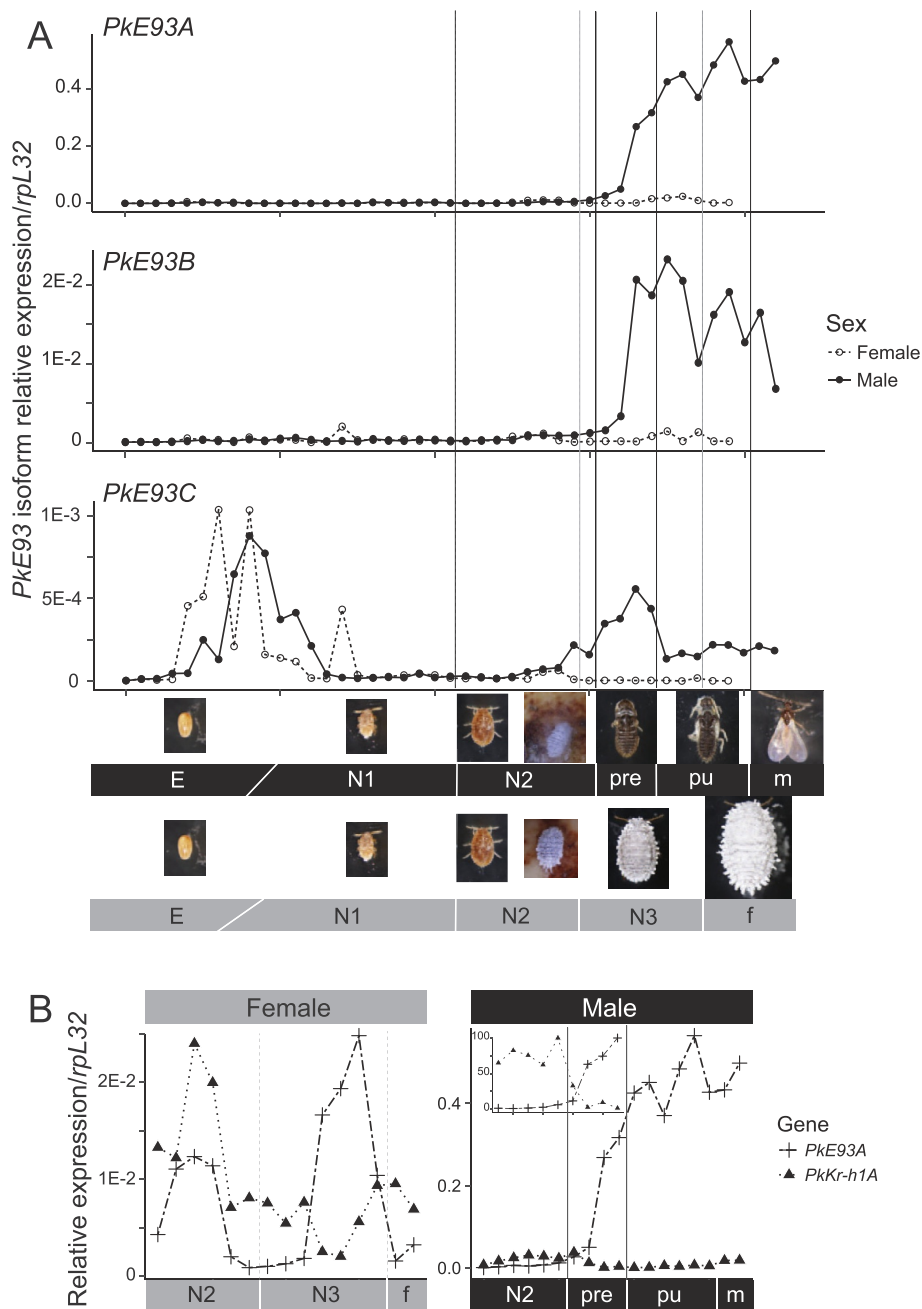


Fig. 2. Expression profiles of *Pke93* isoforms throughout post-oviposition in males and females, and comparison with those of *PkKr-h1A* at the end of development. **A.** *Pke93A*, *Pke93B* and *Pke93C* expression profiles from qRT-PCR of samples collected every 24 h from oviposition. The primers used for qRT-PCR are shown in Fig. 1 and their sequences are listed in Table S1. **B.** Comparison of *Pke93A* and *PkKr-h1A* expression from the second-instar nymph, when female and male can be differentiated, to the adult stage. The inset of male expression graph shows the relative expression in percentage when the switch of expression occurs between the two genes. Photos of each developmental stage were modified from Fig. 1 in Vea et al. (2016) except N3 and f.

2002) and highly conserved (Fig. 1A). Using 5' and 3' RACE PCR combined to primers designed from the conserved region, we cloned and sequenced three complete transcripts of 5008, 5056 and 5233 bp long. All of them resulted from either usage of different transcription initiation site and/or alternative splicing on 5' end only (Fig. 1B). Each isoform was arbitrarily designated as *Pke93A*, *Pke93B* and *Pke93C*. The translated region common to all transcripts counts 1050 aa, *Pke93A* and *Pke93C* predicted protein sequence is of 1050 aa, while *Pke93B* has a predicted protein sequence of 1090 aa. In summary, *Pke93A* and *Pke93C* differ in the 5' untranslated region, while *Pke93B* has a longer coding region.

3.2. Sex-specific expression profiles of *E93*

We first examined the expression profile of each *Pke93* isoform during the post-oviposition development in male and female mealybugs, using absolute qRT-PCR (Fig. 2A). *Pke93A* isoform has the highest

expression compared to the two other isoforms. Generally, *Pke93A* stays at low levels in the embryo, N1 and N2 in both males and females (Fig. 2A; top). In males only, *Pke93A* suddenly increases at the beginning of prepupa and reaches a peak of expression before adult metamorphosis. In females, however, *Pke93A* does not show such dramatic expression, although slight increases at the end of N2 and N3 are observed (Fig. 2B). *Pke93B* isoform followed a similar expression pattern although around 20-fold lower (Fig. 2A; middle), which suggests that *Pke93B* may be a minor isoform. Finally, *Pke93C*, despite its also lower expression, shows a distinct pattern during the embryonic stage (Fig. 2A; bottom), with peaks of expression in both males and females, similar to that of *PkKr-h1* (Fig. S1). At the end of N2, *Pke93C* expression also increases in males but decreases during the pupal stage, while its expression reaches near-zero levels after N2 in females. *Pke93* expression differs between males and females more strikingly than the early JH-response gene *PkKr-h1*. This is especially true towards the end of post-embryonic development, where a peak of expression is observed in

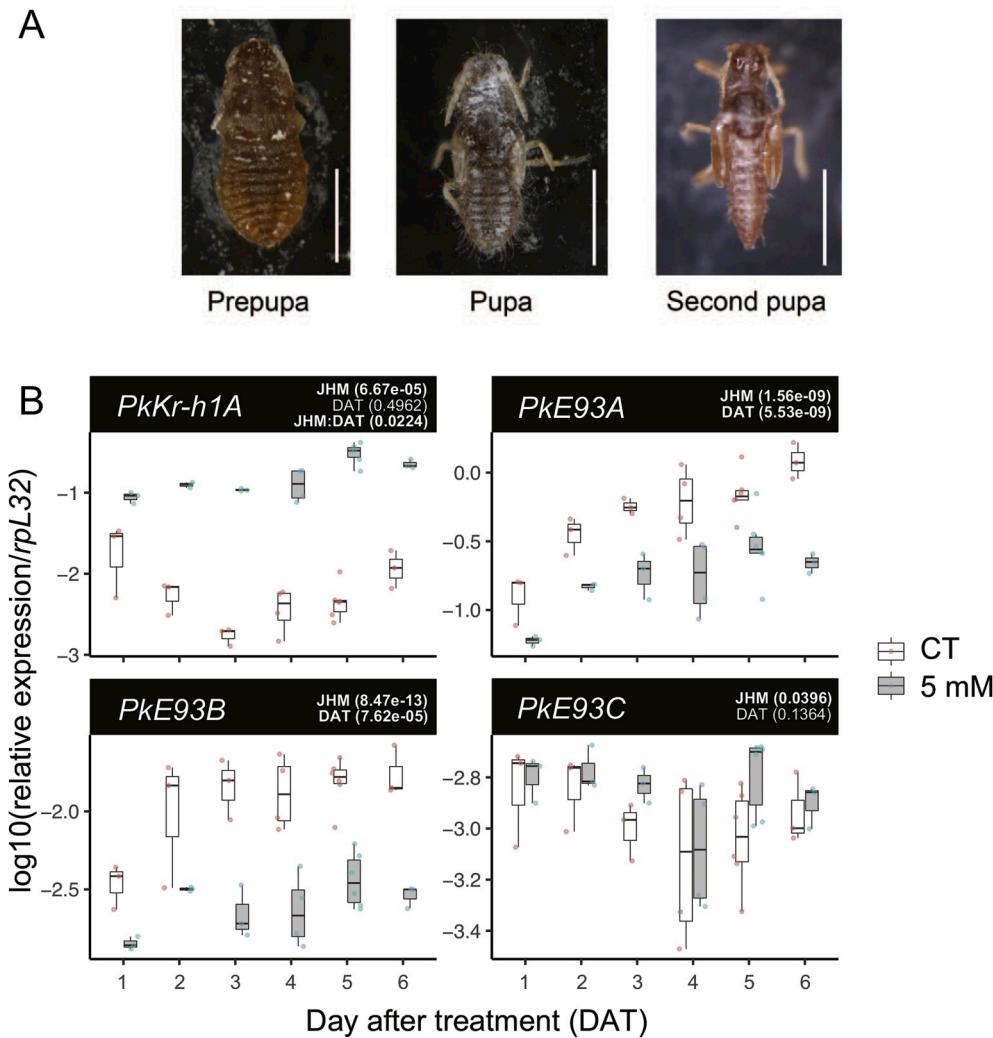


Fig. 3. Effect of juvenile hormone mimic treatment on *Kr-h1* and *E93* expression at the end of male development. **A.** Photos of the dorsal view of prepupa and pupa during the normal life cycle, and second pupa induced 3–4 days after pyriproxyfen application. The phenotype of the second pupa is similar to the adult male, with a more elongated body, neck constriction and longer antennae, but the wings buds are still underdeveloped and similar to the normal pupa. Scale: 500 μ m. **B.** Expression of *PkKr-h1A*, *PkE93A*, *PkE93B* and *PkE93C*, 1–6 days after 1 day old male prepupae (PreD1) were treated with 5 mM pyriproxyfen (5 mM) or methanol (CT). Transcript levels were obtained with qRT-PCR, values normalized with the reference gene *rpL32* levels and log₁₀ transformed. All data points were directly plotted (colored points) as well as a summary of these values with box-and-whisker plots (where the thick line represents the median, the box edges are the upper and lower quartiles, and black dots are outliers). Statistical significance: P-values for each predictor (see Materials and Methods section 2.5) are indicated on top right side of each graph. If the interaction is significant, the p-values of predictors treatment (JHM), time (day after treatment: DAT) and interaction between them (JHM:DAT) are indicated (as it is the case for *PkKr-h1A*). P-values for treatment and day after treatment only (for all three *PkE93* isoforms) are indicated when no significant interaction was found. We considered an effect significant when p-value < 0.01, significant effects have their p-values in bold. (For interpretation of the references to color in this figure legend, the reader is referred to the Web version of this article.)

males, but not in females. At this point, males enter quiescent stages (prepupa and pupa) where wings develop. In contrast, females molt only once then become reproductively mature but retain juvenile features. Along with previous results on *PkKr-h1* and *Pkbr* (Vea et al., 2016), we suggest that sex-specific expression patterns of *PkE93* may contribute to the development of sexual dimorphism in mealybugs.

3.3. Expression pattern of male mealybugs consistent with JH signaling of other insects

The origin of holometaboly has been debated for decades, particularly to establish homology among the developmental stages in hemimetabolous and holometabolous insects. Although a consensus that endocrinological changes are most likely responsible for the transition between hemimetaboly and holometaboly, two main hypotheses were proposed: (1) the Berlese or pronymphal hypothesis emphasizes that differential hatching time led to the origin of various types of metamorphosis during insect evolution (supported by endocrine studies in (Truman and Riddiford, 1999)); and (2) the holometabolous pupal stage emerged from the last nymphal stage in hemimetabolous groups (Hinton, 1963; Sehna et al., 1996). For more details on the history of these two hypotheses, see reviews (Belles, 2011; Rédei and Štys, 2016; Truman and Riddiford, 1999). In the last couple of decades, molecular studies on JH regulation provided additional evidence to support each of these hypotheses. The study of *broad* expression pattern and function in hemimetabolous *Oncopeltus* provided support to the pronymphal hypothesis: *broad* differential growth function during late embryonic

stage of hemimetabolous insects was transposed to the penultimate postembryonic molt in holometabolous insects (Erezyilmaz et al., 2006). However, studies based on other JH-dependent factors also support the latter hypothesis. In fact, the expression pattern of JH-dependent *Kr-h1* suggests that the last nymphal stage in hemimetabolous *Pyrrhocoris* may be homologous to the pupal stage in holometabolous *Tribolium* (Konopova et al., 2011). Moreover, late post-embryonic developmental expression pattern and knockdown of *E93* in *B. germanica* support this homology statement (Ureña et al., 2014), especially with links to JH signaling pathway (Belles and Santos, 2014; Ureña et al., 2016). Finally, the propupal and pupal stages in neometabolous Thysanoptera, could be together homologous to the holometabolous pupal stage (Minakuchi et al., 2011).

A similar neometabolous development occurs in male scale insects (stages traditionally coined as “prepupa” and “pupa”). We previously presented that hormonal treatment using JHM at the beginning of the male prepupal stage, when *Kr-h1* expression normally drops suddenly, prevents adult metamorphosis and creates a supernumerary pupal stage that we call second pupa (Fig. 3A) (Vea et al., 2016). The first pupa emerges 3 or 4 days after treatment, followed by second pupa 3 days later, while the control pupa also emerges 3 or 4 days after treatment but stays at this stage for around 5–7 days before molting to the adult stage (Table S2). The supernumerary stage emerges earlier but adult metamorphosis never happens (Vea et al., 2016). In this study, we further show that *PkE93* expression in male *P. kraunhia* starts at the beginning of the prepupa and peaks at the beginning of the pupal stage (Fig. 2A). In addition to maintaining high levels of *PkKr-h1* for at least

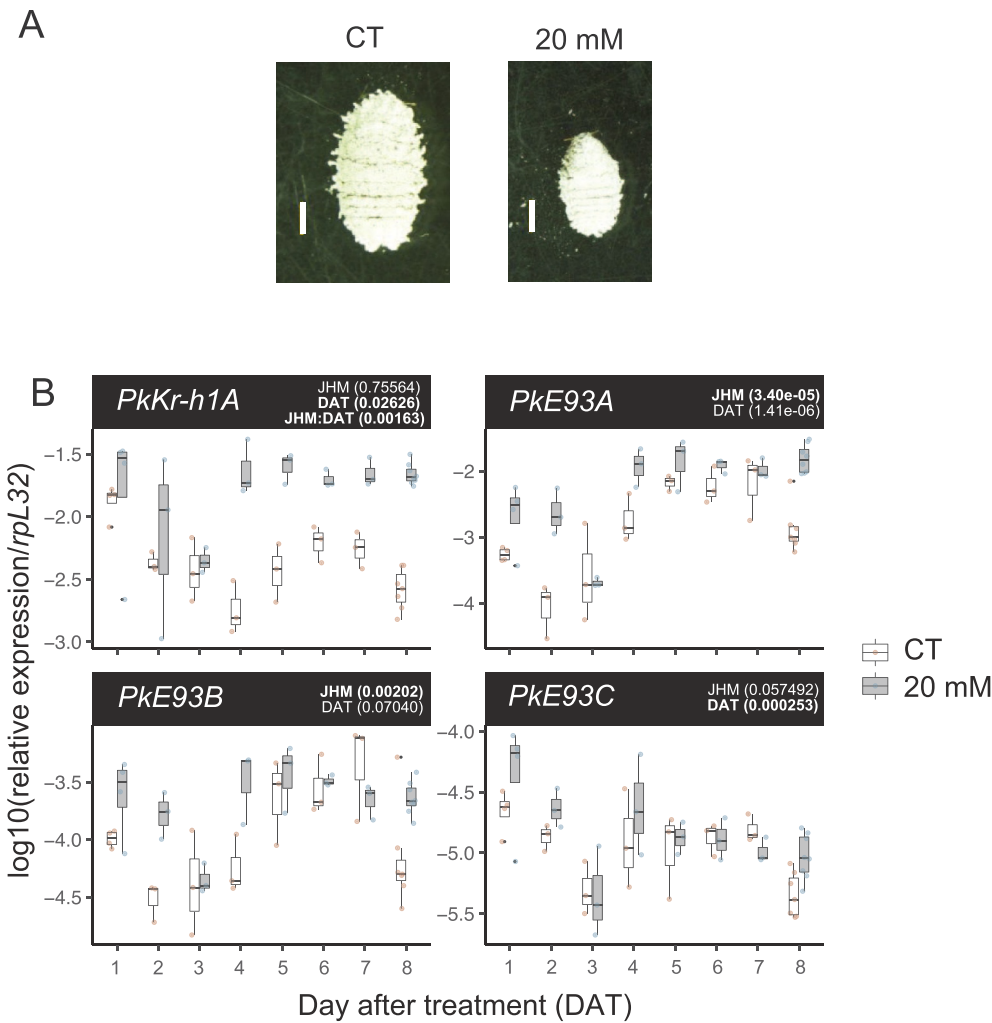


Fig. 4. Effect of juvenile hormone mimic treatment on *Kr-h1* and *E93* expression at the end of female development. **A.** Dorsal view of the adult females 25 days after treatment with methanol (CT) and 20 mM pyriproxyfen (20 mM). JHM did not have an effect on the general shape of the adult females. JHM treated females were significantly smaller in size. Scale: 200 μ m. **B.** Expression of *PkKr-h1A*, *PkE93A*, *PkE93B* and *PkE93C*, 1–8 days after 0–24 h old third instar females (N3D0) were treated with 20 mM pyriproxyfen or methanol. The transcript levels were analyzed with qRT-PCR, normalized with the *rpL32* levels, and log₁₀ transformed. All data points were directly plotted (colored points) as well as a summary of these values with box-and-whisker plots (where the thick line represents the median, the box edges are the upper and lower quartiles, and black dots are outliers). Statistical significance: P-values for each predictor (see Materials and Methods section 2.5) are indicated on top right side of each graph. If the interaction is significant, the p-values of predictors treatment (JHM), time (day after treatment: DAT) and interaction between them (JHM:DAT) are indicated (as it is the case for *PkKr-h1A*). P-values for treatment and day after treatment only (for all three *PkE93* isoforms) are indicated when no significant interaction was found. We considered an effect significant when p-value < 0.01; significant effects have their p-values in bold.

six days, JHM treatment results in the significant decrease of *PkE93A* and *PkE93B*, while *PkE93C* is not significantly affected (Fig. 3A).

Although functional analyses are still necessary to confirm this in mealybugs, the effects of JHM on *E93* expression in neometabolous males are congruent with previous results found in other holometabolous and hemimetabolous insect, where a peak of *E93* expression is necessary during the last preimaginal stage to induce adult metamorphosis. Additionally, we show in the case of this neometabolous Hemiptera that maintaining the transcription of JH-dependent *Kr-h1* leads to the creation of an additional pupal stage.

3.4. Atypical regulation of JH signaling and *E93* in female mealybugs

Based on *PkE93* expression profiles in females, all isoforms transcripts remain very low throughout the successive molting events, contrasting with male neometabolous development. However, if we compare *PkE93* and *PkKr-h1* expression only during the last instar nymphs, we see that even at very low levels, a slight decrease of *PkKr-h1* is accompanied with a small peak of expression of *PkE93A* (Fig. 2B) and this change is significant at least with *PkE93A* based on its expression in control treatments of females (see p-value of DAT in Fig. 4B, which indicates a significant change in expression over days). Although the female expression is 20-fold lower than in males, this small peak could explain sexual maturation in females after N3, while somatic differentiation does not occur in the imago (see Fig. 2A, photos of female developmental stages). A recent study on *E93* expression in neotenic females of holometabolous Strepsiptera *Xenos vesparum* revealed

that *XvE93* low expression was linked to neotenic abdomen, while the cephalothorax expresses *XvE93* (Chafino et al., 2018). Although we could not confirm tissue-specific expression of *PkE93* due to the minute size of mealybug nymphal ovaries, future RNA *in situ* hybridization may show similar tissue-specific expression patterns.

JH presence during the nymphal stages is anti-metamorphic and a drop of its level is essential for adult transition (Jindra et al., 2013). In male mealybugs, we see the levels of *PkKr-h1* decrease rapidly at the end of N2. However in females, at the same stage, JH is almost absent. We decided to test whether females undergo neotenic development as a result of not attaining the minimum JH-level threshold to pursue the same type of adult metamorphosis as their male counterparts. As *PkKr-h1* expression begins to decrease progressively at the penultimate nymphal stage in females (Fig. 2B and Fig. S1; Vea et al., 2016), we applied JHM at the early last nymphal stage (N3D0). By doing so, we assessed whether *Kr-h1* needs to reach a specific threshold necessary for the switch to adult fate controlled by *E93*. Twenty mM of pyriproxyfen were applied on N3D0, a concentration four times higher than male treatments. Following this treatment, 7 out of 19 (37%) treated individuals died before the last molt (Table 1). The 12 survivors (63%) showed a tendency to prolong the final nymphal stage (N3). While the control samples molted 9.6 ± 1.5 days ($N = 14$) after treatment, 12 out of 19 JHM-treated individuals molted to adult stage 13 ± 2.5 days after treatment. After the final molt, JHM-treated females were smaller than the control (Fig. 4A).

We followed the effect of JHM treatment on *PkKr-h1* and *PkE93* expression (Fig. 4B) one to eight days after treatment (last days before

Table 1
Effect of pyriproxyfen treatment on last nymphal instar females on adult metamorphosis.

	N	Number of dead individuals during N3 (%)	Number of individuals alive that molted to adult (%)									
			8	9	10	11	12	13	14	15	16	(days after treatment)
Methanol	14	0 (0)	3 (21)	6 (43)	1 (7.1)	3 (21)	0 (0)	1(7.1)	0 (0)	0 (0)	0 (0)	
20 mM pyriproxyfen	19	7 (37)	0 (0)	2 (11)	1 (5.3)	1 (5.3)	0 (0)	5 (26)	0 (0)	0 (0)	3 (16)	

the female adult molt). At 20 mM, pyriproxyfen induced the up-regulation of *PkKr-h1* after four days, which then lasted several days. However, it is worth mentioning that *PkKr-h1* levels were significantly lower than the response observed in males (Fig. 3B), even with a concentration of pyriproxyfen four times higher. We suggest that female mealybugs may possess mechanisms preventing them to respond to JH as sensitively or efficiently as in males, at least during their development. Previously, we showed that *PkMet* and *PkTai*, forming the JH receptor complex, were highly expressed at the end of male development, while in females the expression remained low (Vea et al., 2016). After JHM treatment on females at N3D0, although *PkKr-h1* starts to be affected only four days after treatment by an upregulation, the expression of all *PkE93* isoforms does not change significantly over time (interaction between treatment and time not significant; Fig. 4B). However, when removing the interaction, the treatment alone leads to an overall significant effect for two isoforms; this is probably explained by the increase in expression at Day 2, Day 4 and Day 8 after treatment for *PkE93A* and *PkE93B*. We therefore conclude that applying JHM on early ultimate juvenile instars in females does not significantly change *PkE93* expression over time, but a small effect might be observed at Day 8 after treatment by an increase of *PkE93A* and *PkE93B*. Overall, in the case of female development, attempting to increase JH levels did not induce a high peak of expression of *PkE93*, as hypothesized.

In mealybugs, males and females are phenotypically identical until the middle of N2. In females, *PkKr-h1* down-regulation takes place in a progressive manner starting from the middle of N2. Moreover, *Pkjhamt* (juvenile hormone acid O-methyltransferase), involved in the last steps of JH biosynthesis, starts decreasing even at the beginning of N2, while in males, the transcripts are still expressed until prepupa (Vea et al., 2016). This indicates an early arrest in JH synthesis in female development. A possibility is that reaching a threshold of *PkKr-h1* transcripts followed by a sudden decrease in expression are both necessary to induce *E93* expression. In this case, maintaining low levels of *PkKr-h1* during female development may explain why *PkE93* expression never peaks.

4. Concluding remarks

The anti-metamorphic role of JH in insect metamorphosis suggests that high levels of this hormone delays metamorphosis. Female neoteny has therefore been believed to be the result of disrupted JH down-regulation leading to constantly high JH titers. Although this hypothesis was first proposed based only on the differential size of scale insect *corpura allata* (Matsuda, 1976), we recently reported contradictory evidence that the last juvenile stages in the female Japanese mealybug develop under surprisingly lower JH titers compared to males (Vea et al., 2016). In this study, we provide additional data to support an atypical hormonal regulation in mealybugs, and show the first example of possible failure in *E93* induction, possibly leading to neotenic reproductive females in an hemimetabolous insect. The response of female development to JH modulations is intriguing and suggests that mealybug neotenic forms are insensitive to JH signaling as opposed to males, which in turn affects *E93* expression, and leads to extreme sexual dimorphism. So far, gene expression manipulation on mealybug juvenile stages by dsRNA injection has been ineffective. Alternatively, identifying suppressors of *E93* promoter in neotenic females, coupled

with functional studies through genome editing should provide novel insights on the function and interaction between *E93* and JH signaling pathway in neotenic female scale insects.

Acknowledgements

We thank Jun Tabata for providing the Japanese mealybugs, Ken Miura and Xavier Belles for their valuable comments on this study. All the work presented here was conducted at Nagoya University and was funded by a Japan Society for the Promotion of Science (JSPS) post-doctoral fellowship for overseas researchers to IMV and a Grant-in-aid for Scientific Research (15K07791) to CM from JSPS.

Appendix A. Supplementary data

Supplementary data to this article can be found online at <https://doi.org/10.1016/j.ibmb.2018.11.008>.

References

- Baehrecke, E.H., Thummel, C.S., 1995. The *Drosophila* *E93* gene from the 93F early puff displays stage- and tissue-specific regulation by 20-hydroxyecdysone. *Dev. Biol.* 171, 85–97. <https://doi.org/10.1006/dbio.1995.1262>.
- Belles, X., 2011. Origin and evolution of insect metamorphosis. In: *encyclopedia of Life Sciences*. John Wiley & Sons, Ltd, Chichester, UK. <https://doi.org/10.1002/9780470015902.a0022854>.
- Belles, X., Santos, C.G., 2014. The MEKRE93 (Methoprene tolerant-Krüppel homolog 1-E93) pathway in the regulation of insect metamorphosis, and the homology of the pupal stage. *Insect Biochem. Mol. Biol.* 52, 60–68. <https://doi.org/10.1016/j.ibmb.2014.06.009>.
- Bocakova, M., Bocak, L., Hunt, T., Teraväinen, M., Vogler, A.P., 2007. Molecular phylogenetics of Elateriformia (Coleoptera): evolution of bioluminescence and neoteny. *Cladistics* 23, 477–496. <https://doi.org/10.1111/j.1096-0031.2007.00164.x>.
- Buszczak, M., Segaves, W.A., 2000. Insect metamorphosis: out with the old, in with the new. *Curr. Biol.* 10, R830–R833. [https://doi.org/10.1016/S0960-9822\(00\)00792-2](https://doi.org/10.1016/S0960-9822(00)00792-2).
- Chafino, S., Lopez-Escardo, D., Benelli, G., Kovac, H., Casacuberta, E., Franch-Marro, X., Kathirithamby, J., Martin, D., 2018. Differential expression of the adult specifier *E93* in the strepsipteran *Xenos vesparum* Rossi suggests a role in female neoteny. *Sci. Rep.* 14176. <https://doi.org/10.1038/s41598-018-32611-y>.
- Danzig, E.M., 1980. Coccids of the Far Eastern USSR (Homoptera, Coccinea) with Phylogenetic Analysis of Coccids in the World Fauna. Nauka, Leningrad.
- Erezyilmaz, D.F., Hayward, A., Huang, Y., Paps, J., Acs, Z., Delgado, J.A., Collantes, F., Kathirithamby, J., 2014. Expression of the pupal determinant broad during metamorphic and neotenic development of the strepsipteran *Xenos vesparum* Rossi. *PLOS ONE* 9, e93614. <https://doi.org/10.1371/journal.pone.0093614>.
- Erezyilmaz, D.F., Riddiford, L.M., Truman, J.W., 2006. The pupal specifier broad directs progressive morphogenesis in a direct-developing insect. *Proc. Natl. Acad. Sci. U.S.A.* 103, 6925–6930. <https://doi.org/10.1073/pnas.0509983103>.
- Gould, S.J., 1977. *Ontogeny and Phylogeny*. Harvard University Press.
- Gómez-Rubio, V., 2017. ggplot2- elegant graphics for data analysis (2nd edition). *J. Stat. Software* 77. <https://doi.org/10.18637/jss.v077.b02>.
- Grimaldi, D., Engel, M.S., 2005. *Evolution of the Insects*, first ed. Cambridge University Press, New York.
- Gujar, H., Palli, S.R., 2016. Krüppel homolog 1 and *E93* mediate juvenile hormone regulation of metamorphosis in the common bed bug, *Cimex lectularius*. *Sci. Rep.*, 26092. <https://doi.org/10.1038/srep26092>.
- Gullan, P.J., Kosztarab, M., 1997. Adaptations in scale insects. *Annu. Rev. Entomol.* 42, 23–50. <https://doi.org/10.1146/annurev.ento.42.1.23>.
- Higashi, M., Abe, T., 1997. Global diversification of termites driven by the evolution of symbiosis and sociality. In: *Biodiversity*. Springer, New York, NY, New York, NY, pp. 83–112. https://doi.org/10.1007/978-1-4612-1906-4_7.
- Hinton, H.E., 1963. The origin and function of the pupal stage. *Proceedings of the Royal Entomological Society of London. Series A, General Entomology* 38, 77–85. <https://doi.org/10.1111/j.1365-3032.1963.tb00759.x>.
- Hodin, J., Riddiford, L.M., 2000. Parallel alterations in the timing of ovarian ecdysone receptor and ultraspiracle expression characterize the independent evolution of larval reproduction in two species of gall midges (Diptera: Cecidomyiidae). *Dev. Gene. Evol.* 210, 358–372. <https://doi.org/10.1007/s004270050324>.

- Jindra, M., Belles, X., Shinoda, T., 2015. Molecular basis of juvenile hormone signaling. *Curr. Opin. Insect Sci.* 11, 39–46. <https://doi.org/10.1016/j.cois.2015.08.004>.
- Jindra, M., Palli, S.R., Riddiford, L.M., 2013. The juvenile hormone signaling pathway in insect development. *Annu. Rev. Entomol.* 58, 181–204. <https://doi.org/10.1146/annurev-ento-120811-153700>.
- Kathirithamby, J., 2009. Host-parasitoid associations in Strepsiptera. *Annu. Rev. Entomol.* 54, 227–249. <https://doi.org/10.1146/annurev.ento.54.110807.090525>.
- Kayukawa, T., Jouraku, A., Ito, Y., Shinoda, T., 2017. Molecular mechanism underlying juvenile hormone-mediated repression of precocious larval-adult metamorphosis. *Proc. Natl. Acad. Sci. U. S. A.* 114, 1057–1062. <https://doi.org/10.1073/pnas.1615423114>. 201615423.
- Kiss, I., Beaton, A.H., Tardiff, J., Fristrom, D., Fristrom, J.W., 1988. Interactions and developmental effects of mutations in the Broad-Complex of *Drosophila melanogaster*. *Genetics* 118, 247–259.
- Konopova, B., Jindra, M., 2008. Broad-Complex acts downstream of Met in juvenile hormone signaling to coordinate primitive holometabolous metamorphosis. *Development* 135, 559–568. <https://doi.org/10.1242/dev.016097>.
- Konopova, B., Smykal, V., Jindra, M., 2011. Common and distinct roles of juvenile hormone signaling genes in metamorphosis of holometabolous and hemimetabolous insects. *PLoS One* 6, e28728. <https://doi.org/10.1371/journal.pone.0028728>.
- Koteja, J., 1990. Life history. In: *Armored Scale Insects, Their Biology, Natural Enemies, and Control*. Vol. a Elsevier, New York, NY.
- Lee, C.Y., Wendel, D.P., Reid, P., Lam, G., Thummel, C.S., Baehrecke, E.H., 2000. E93 directs steroid-triggered programmed cell death in *Drosophila*. *Mol. Cell.* 6, 433–443.
- Matsuda, R., 1976. *Morphology and Evolution of the Insect Abdomen: with Special Reference to Developmental Patterns and Their Bearings upon Systematics*. Pergamon Press.
- Minakuchi, C., Tanaka, M., Miura, K., Tanaka, T., 2011. Developmental profile and hormonal regulation of the transcription factors *broad* and *Krüppel homolog 1* in hemimetabolous thrips. *Insect Biochem. Mol. Biol.* 41, 125–134. <https://doi.org/10.1016/j.ibmb.2010.11.004>.
- Mou, X., Duncan, D.M., Baehrecke, E.H., Duncan, I., 2012. Control of target gene specificity during metamorphosis by the steroid response gene E93. *Proc. Natl. Acad. Sci. U.S.A.* 109, 2949–2954. <https://doi.org/10.1073/pnas.1117559109>.
- Parthasarathy, R., Tan, A., Bai, H., Palli, S.R., 2008. Transcription factor broad suppresses precocious development of adult structures during larval-pupal metamorphosis in the red flour beetle, *Tribolium castaneum*. *Mech. Dev.* 125, 299–313. <https://doi.org/10.1016/j.mod.2007.11.001>.
- Rédei, D., Štys, P., 2016. Larva, nymph and naiad - for accuracy's sake. *Syst. Entomol.* 41, 505–510. <https://doi.org/10.1111/syen.12177>.
- Roisin, Y., 2000. Diversity and evolution of caste patterns. In: *Termites: Evolution, Sociality, Symbioses, Ecology*. Springer, Dordrecht, Dordrecht, pp. 95–119. https://doi.org/10.1007/978-94-017-3223-9_5.
- Roy, S., Saha, T.T., Zou, Z., Raikhel, A.S., 2018. Regulatory pathways controlling female insect reproduction. *Annu. Rev. Entomol.* 63, 489–511. <https://doi.org/10.1146/annurev-ento-020117-043258>.
- Saiki, R., Gotoh, H., Toga, K., Miura, T., Maekawa, K., 2015. High juvenile hormone titre and abdominal activation of JH signalling may induce reproduction of termite neotenic. *Insect Mol. Biol.* 24, 432–441. <https://doi.org/10.1111/imb.12169>.
- Sehnal, F., Švacha, P., Zrzavý, J.Z., 1996. Evolution of insect metamorphosis. In: Gilbert, L.I., Tata, J.R., Atkinson, B.G. (Eds.), *METAMORPHOSIS*. Academic Press Inc., pp. 3–58. <https://doi.org/10.1016/b978-012283245-1/50003-8>.
- Siegmund, T., Lehmann, M., 2002. The *Drosophila* Pipsqueak protein defines a new family of helix-turn-helix DNA-binding proteins. *Dev. Gene. Evol.* 212, 152–157. <https://doi.org/10.1007/s00427-002-0219-2>.
- South, A., Stanger-Hall, K., Jeng, M.-L., Lewis, S.M., 2011. Correlated evolution of female neoteny and flightlessness with male spermatophore production in fireflies (Coleoptera: Lampyridae). *Evolution* 65, 1099–1113. <https://doi.org/10.1111/j.1558-5646.2010.01199.x>.
- Sugahara, R., Minaba, M., Jouraku, A., Kotaki, T., Yamamoto, T., Shinohara, Y., Miyoshi, H., Shiotsuki, T., 2016. Characterization of two adenine nucleotide translocase paralogues in the stink bug, *Plautia stali*. *J. Pestic. Sci.* 41, 44–48.
- Truman, J.W., Riddiford, L.M., 2002. Endocrine insights into the evolution of metamorphosis in insects. *Annu. Rev. Entomol.* 47, 467–500. <https://doi.org/10.1146/annurev.ento.47.091201.145230>.
- Truman, J.W., Riddiford, L.M., 1999. The origins of insect metamorphosis. *Nature* 401, 447–452. <https://doi.org/10.1038/46737>.
- Uhlířova, M., Foy, B.D., Beaty, B.J., Olson, K.E., Riddiford, L.M., Jindra, M., 2003. Use of Sindbis virus-mediated RNA interference to demonstrate a conserved role of Broad-Complex in insect metamorphosis. *Proc. Natl. Acad. Sci. U.S.A.* 100, 15607–15612. <https://doi.org/10.1073/pnas.2136837100>.
- Ureña, E., Chafino, S., Manjón, C., Franch-Marro, X., Martín, D., 2016. The occurrence of the holometabolous pupal stage requires the interaction between E93, Krüppel-Homolog 1 and Broad-Complex. *PLoS Genet.* 12, e1006020. <https://doi.org/10.1371/journal.pgen.1006020>.
- Ureña, E., Manjón, C., Franch-Marro, X., Martín, D., 2014. Transcription factor E93 specifies adult metamorphosis in hemimetabolous and holometabolous insects. *Proc. Natl. Acad. Sci. U.S.A.* 111, 7024–7029. <https://doi.org/10.1073/pnas.1401478111>.
- Veá, I.M., Tanaka, S., Shiotsuki, T., Jouraku, A., Tanaka, T., Minakuchi, C., 2016. Differential juvenile hormone variations in scale insect extreme sexual dimorphism. *PLOS ONE* 11, e0149459. <https://doi.org/10.1371/journal.pone.0149459>.